Available online at www.sciencedirect.com
ScienceDirect
Mendeleev Commun., 2014, **24**, 308–310

Mendeleev Communications

Non-steady propagation of single and counter hydrogen and methane flames in initially motionless gas

Nikolai M. Rubtsov,*[a] Boris S. Seplyarskii,[a] Ideya M. Naboko,[b] Victor I. Chernysh,[a] Georgii I. Tsvetkov[a] and Kirill Ya. Troshin[c]

[a] *Institute of Structural Macrokinetics and Materials Science, Russian Academy of Sciences, 142432 Chernogolovka, Moscow Region, Russian Federation. Fax: +7 495 962 8025; e-mail: nmrubtss@mail.ru*
[b] *Joint Institute of High Temperatures, Russian Academy of Sciences, 127412 Moscow, Russian Federation. E-mail: idnaboko@yandex.ru*
[c] *N. N. Semenov Institute of Chemical Physics, Russian Academy of Sciences, 119991 Moscow, Russian Federation*

DOI: 10.1016/j.mencom.2014.09.021

An increase in warming up in the combustion of hydrocabons with simultaneous initiation at opposite butt-ends of a cylindrical reactor by a factor of ~2, as compared to flame propagation from a single initiation source, is due to the two-stage combustion process.

Gas explosions in pipes are closely related to the problems of explosion safety and verification of general flame propagation mechanisms, in particular, with flame acceleration and transition from deflagration to detonation. The flame shape in the course of propagation to the end of a pipe changes from convex (towards unreacted mixture) to concave one;[1–3] it is known as flame inversion.[2] Mechanisms of flame propagation in pipes and interrelation between acoustic fluctuations and flame front (FF) velocity were analysed.[4] A flat FF is unstable,[5] hydrodynamic instability provides a cellular or folded FF shape. Note that a propagating FF is not defined by a single characteristic acoustic frequency, but a set of frequencies, which cause origination of flame instability areas, thus their boundaries are displaced with a change of acoustic amplitude.[6]

The mutual influence of spherical counter flames was studied.[7] Due to a limited volume of experimental data, the interaction of FF originated upon transition from a spherical flame to propagation in a cylinder was not considered. The propagation of a counter FF caused by simultaneous initiation at opposite butt-ends of a cylindrical reactor leads to higher pressure increase by a factor of ~2 than that at FF propagation from a single initiation source.[8] The experiments were performed in the presence of a planar meshed obstacle. Under these conditions, the existence of two stages of the kinetic mechanism of natural gas combustion was observed. The first stage corresponded to the propagation of a cool blue front of incomplete chemical conversion (due to the $CH_4 \rightarrow CO$ transformation); the second stage is due to the fast chemical transformation of the products of incomplete oxidation of natural gas (due to the $CO \rightarrow CO_2$ transformation), and it occurred under the conditions of initiation at both bott-ends.

The aim of this work was to study propagation of both single and counter FFs of hydrogen and natural gas (NG) mixtures with O_2 and air in closed cylindrical reactors of various diameters under different conditions of spark initiation in initially motionless gas by means of high speed cinematography.[†]

(a) (b) (c)

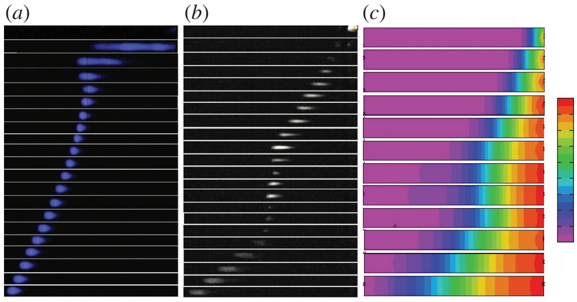

The degree of advancement of one-step reaction

Figure 1 Consecutive frames of flame propagation in cylindrical quartz reactor 1: (*a*) 50% (33% NG + 67% O_2) + 50% CO_2, P = 200 Torr, 60 frames s^{-1}; (*b*) 50% (15% H_2 + 85% O_2) + 45% CO_2 + 4% CCl_4, P = 200 Torr, 60 frames s^{-1}; (*c*) calculation of flame propagation ($L_x = 10L_y$) with the use of system I [equations (1a)–(1g), see Online Supplementary Materials], one activated reaction.

Typical results of high-speed filming of FF propagation in reactor 1 are presented in Figure 1. The FF propagates with a variable speed, both in hydrogen and NG combustion. Therefore, the non-steady FF propagation is not due to the kinetic mechanism of combustion because the kinetics of the reactions differ

[†] The experiments were performed in quartz cylindrical reactors of 30 mm (reactor 1) and 40 mm (reactor 2) in diameter and 1000 mm long; in a reactor of 140 mm in diameter and 700 mm long[8] (reactor 3) at total pressures up to 300 Torr. Experiments at 1 atm were performed in a stainless steel reactor of 25 cm in length and 12 cm in diameter supplied with an optical quartz window of 12 cm in diameter at the butt-end (reactor 4). The pumped out reactors were filled with a preliminarily prepared gas mixture up to a necessary pressure; initiation was provided by a spark discharge (1.5 J in reactors 1,3,4 and 0.92 J in reactor 2). Two pairs of spark ignition electrodes were located at opposite butt-ends of reactors 1–3 and located opposite on diameter at a lateral surface of reactor 4 in 12.5 cm from its end faces; the pairs were connected to a power supply consistently to provide two simultaneous discharges. Each pair could be short circuited to provide a single discharge. The speed filming of ignition dynamics and FF propagation was carried out from the sides of reactors 1–3 and from the end face of reactor 4 with a Casio Exilim F1 Pro color high-speed digital camera (frames frequency of 60–1200 s^{-1}).[9] The filming was turned on at an arbitrary moment before initiation. The video file was stored in computer memory and its time-lapse processing was performed.[10] CCl_4 was added to H_2–O_2 (air) mixtures to visualize FF;[9] the additive up to 4% CCl_4 is inert for hydrogen mixtures.[11] NG contained 98.8% methane and 1.2% propane; other reagents were chemically pure. The pressure change in the course of combustion was recorded by a piezoelectric gage synchronized with the discharge.

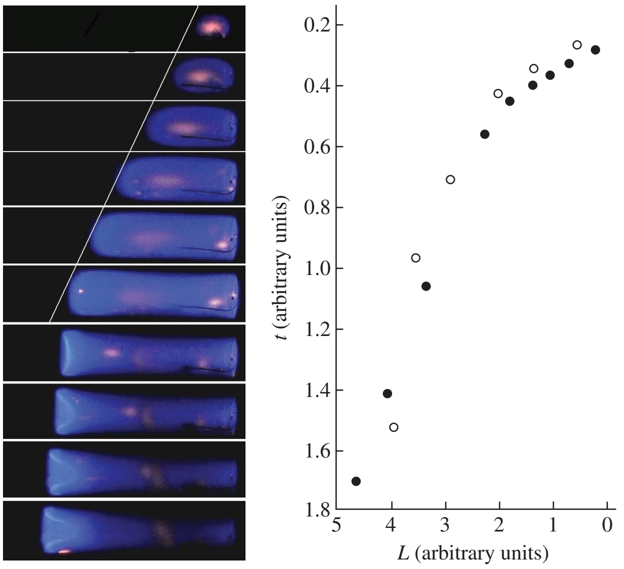

Figure 2 Consecutive frames of FF propagation in 50% (33% NG + 67% O_2) + 50% CO_2, $P = 160$ Torr from the centre of reactor 3, 600 frames s^{-1}. Black points (on the right) – calculations of the time dependence of distance of the FF from an initiation place [*t*–*L* diagram, system I (1a), (1c)–(1h), empty points – (1a)–(1g), see Online Supplementary Materials], one activated reaction.

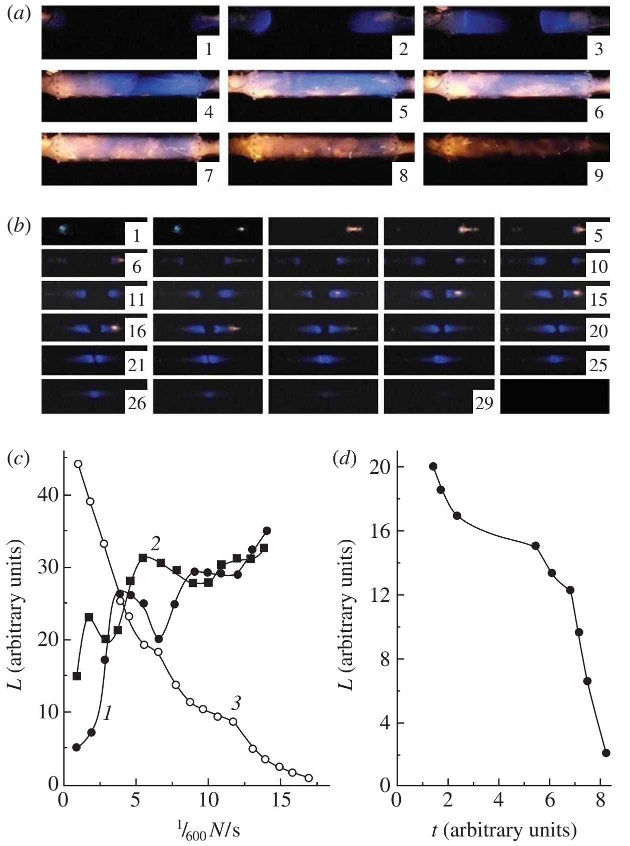

Figure 3 High-speed filming of counter FF propagation: (*a*) 50% (33% NG + + 67% O_2) + 50% Kr, $P = 95$ Torr, 600 frames s^{-1} at simultaneous initiation by a spark at both bott-ends of reactor 2; (*b*) 50% (33% NG + 67% O_2) + + 50% CO_2, $P = 200$ Torr, 60 frames s^{-1} at simultaneous initiation by a spark since both ends of reactor 1. (*c*) Time dependence of (*1*) the distance of the left FF from the left wall of the reactor; (*2*) the distance of the right FF from the right wall of the reactor; (*3*) the distance between FFs. (*d*) Calculated time dependence of distance between FFs in a narrow channel ($L_x = 10L_y$), system I [equations (1a)–(1g), see Online Supplementary Materials], one activated reaction.

essentially. Note that flame propagation with a variable speed was also observed[12] at FF propagation in near-stoichiometric propane–air mixtures at 1 atm in a plexiglass pipe of 40 mm in diameter and 1900 mm long with an open end. This was explained[12] by the interaction of FF with acoustic oscillations in the pipe. The high-speed filming gives an opportunity to control the constancy of FF velocity in a pipe; the use of several one-dimensional sensors (sensors of pressure, ionization sensors) can lead to doubtful results in the measurement of FF velocities.

In Figure 2, a typical result of high-speed filming of single FF propagation initiated at the center of reactor 3 in a mixture of 50% (33% NG + 67% O_2) + 50% CO_2 to the left butt-end is presented. The FF propagation far from the end face occurs with an almost constant velocity; then, in the vicinity of the butt-end, the FF velocity decreases and flame inversion is observed in agreement with published data.[2,9–12] As follows from Figures 1 and 2, non-steady FF propagation is characteristic of narrow pipes;[12] in the wider pipe 140 mm in diameter (reactor 3), such a non-steady flame is not observed; thus, in the vicinity of the end face of the pipe, FF is smoothly slowed down because of gas compression at the reactor end face.

Non-steady FF propagation in a closed tube is especially evidently shown by an example of counter flames [Figure 3(*a*),(*b*)]. In Figure 3, typical results of the high-speed filming of counter flames are presented for both stoichiometric 50% (NG + 2 O_2) + + 50% Kr in the reactor 2 (*a*), and for 50% (NG + 2 O_2) + 50% CO_2 in reactor 1 (*b*). In the fast-burning mixture (*a*) counter flame fronts change the shape in the course of propagation [Figure 3(*a*), shots 2 and 3]. For the mixture diluted with CO_2 [Figure 3(*b*)], the propagation of each flame is non-steady; thus, the distance between counter FF [Figure 3(*c*)] depends on time not smoothly.

Note that if in slowly burning mixture [Figure 3(*b*)] after meeting of FFs the luminescence in the reactor vanishes; however, in the quickly burning mixture [Figure 3(*a*)], the luminescence in the reactor is observed after contact of FF [Figure 3(*a*), shots 5–9]; one can observe a spiral luminescing trace of burning-down gas [Figure 3(*a*), shot 9] at the end of combustion. It means that chemical transformation in gas mixture is incomplete in agreement with published data.[8]

In reactor 3, unsteady combustion is expressed in the occurrence of inverse fronts of counter flames [Figure 4(*a*),(*b*)] though in reactors of smaller diameter flame inversion is less pronounced.[9] FFs at propagation towards each other show an inverse character in turn: the inversion of one of counter flames metamorphoses into an almost flat front of this flame, while the opposite FF becomes inverse. Note that both of the experiments presented in Figure 4 were performed under the same conditions; however, the dynamics of evolution of FF inversion is distinct. It was impossible to reproduce the time history of the inversion of a counter flame under identical experimental conditions though the time of flame meeting remains almost the same. This should be taken into account in numerical calculations of counter flames propagation.

After the meeting of flames, the luminescence in the reactor disappears. In the course of combustion, a bright disk [especially well visible on the right side of shots 30–45, Figure 4(*a*), and shots 36–44, Figure 4(*b*)] is formed behind the FF. The reasons of the occurrence of this disk require further investigations.

The propagation of a counter FF caused by simultaneous initiation from opposite butt-ends of a cylindrical reactor without any obstacles is accompanied by the same pressure increase in comparison with that at FF propagation from the single initiation source. Therefore, the reason for an increase of a warming up at initiation at both butt-ends[8] lies in the fact that, at this initiation in the presence of a meshed obstacle, the fast combustion of

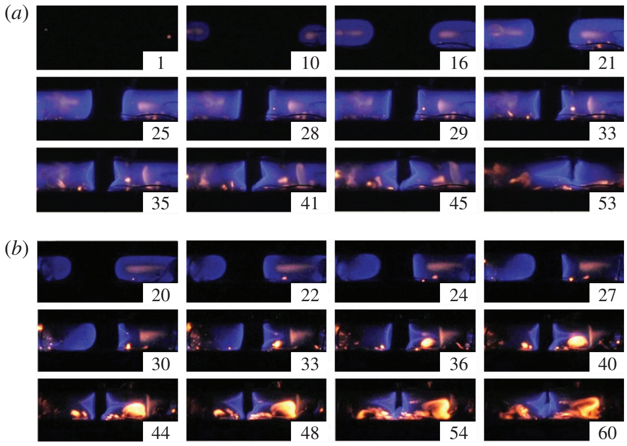

Figure 4 High-speed filming of counter FF propagation in a mixture of 50% (33% NG + 67% O_2) + 50% CO_2, P = 170 Torr, 600 frames s^{-1}, at simultaneous spark initiation at both butt-ends of reactor 3. Experiments (*a*) and (*b*) were performed under the same conditions.

the products of incomplete oxidation of natural gas (hot flame, $CO \rightarrow CO_2$ transformation[11]) occurs as distinct from combustion in the absence of obstacles, when the first stage (blue flame, $CH_4 \rightarrow CO$ transformation[11]) of combustion generally takes place.

To verify the aforesaid the following experiments were performed. It is known that, as opposed to hydrocarbon oxidation, hydrogen oxidation has a simpler kinetic mechanism, in which two consecutive processes as given above cannot be allocated.[11] Figure S1 (Online Supplementary Materials) shows the speed filming of counter (*a*) and single (*b*) FF propagation in a mixture of 4% CCl_4 + 12% H_2 + 84% air at 1 atm under simultaneous spark initiation (*a*) and a single spark ignition (*b*) at a lateral surface of reactor 4. The values of the pressure rise are almost equal both for counter flame propagation and a single flame propagation. Therefore, the increase in the warming-up under double initiation at both butt-ends in comparison with single initiation is possible only in a two-stage exothermic combustion reaction, when an additional initiation source (along with a flame turbulizer) provides the second more exothermic stage.

In our opinion, any comparison of experimentally recorded movement of the flame emission front with the result of numerical modeling is credible only in a qualitative aspect, *e.g.*, on velocity change of movement of the boundary of initial and actively reacting gas, as well as on the shape of this boundary, the degree of its 'smoothness' and perturbations of its structure. The vast majority of kinetic parameters is not accurate enough to draw reliable conclusions on the basis of modeling. The question of completeness of the kinetic mechanism used is always open, *i.e.* whether any important reaction is overlooked. Moreover, as there are no unicity theorems on reactive Navier–Stokes equations, agreement between calculated quantities and experimental ones does not argue for accord between calculation and experiment as there can be other sets of the governing parameters describing the same profiles.

Compressible dimensionless reactive Navier–Stokes equations in the low Mach number approximation (see our previous work[13] and Online Supplementary Materials) suggested[14–18] showed a qualitative consent with experiments.[13]

The results of the numerical analysis are given in Figure 1(*c*) [system (I), single-stage chemical reaction, see Online Supplementary Materials] for a narrow channel ($L_x = 10L_y$; L_y, L_x are the dimensionless channel width and length, respectively). The calculated time dependence of the FF distance from the channel geometric centre (the point of initiation) is shown in Figure 2. The FF smoothly slows down at an approach to the end face of the channel. Numerical analysis shows that the distance between counter FF [Figure 3(*d*)] in the narrow channel ($L_x = 10L_y$) depends not smoothly on time in a qualitative agreement with experimental results [Figure 3(*c*), curve *3*].

Thus, we experimentally observed that flame fronts (including counter FF) in the mixtures of hydrogen (15–30%) and natural gas (30%) with oxygen at total pressures up to 300 Torr in closed cylindrical vessels propagate in a non-steady way. The increase in the warming-up under double initiation at both bott-ends in comparison with single initiation is possible only in a two-stage exothermic combustion reaction, when an additional initiation source (along with flame turbulizer) provides the second more exothermic stage. Modeling based on compressible reactive Navier–Stokes equations at a low Mach number showed a qualitative agreement with experimental data for both a single Arrhenius reaction and a simple chain mechanism.

Online Supplementary Materials

Supplementary data associated with this article can be found in the online version at doi:10.1016/j.mencom.2014.09.021.

References

1 O. C. Ellis and R. V. Wheeler, *J. Chem. Soc.*, 1928, 3215.
2 G. D. Salamandra, T. V. Bazhenova and I. M. Naboko, *Proc. Combust. Inst.*, 1959, **7**, 851.
3 E. H. W. Schmidt, H. Steinecke and U. Neubert, *Proc. Combust. Inst.*, 1952, **4**, 658.
4 H. Guénoche, in *Non-Steady Flame Propagation*, ed. G. H. Markstein, Pergamon, Berlin, 1964, pp. 107–181.
5 L. Landau, *Acta Phys.-Chim. USSR*, 1944, **19**, 77.
6 C. Clanet and G. Searby, *Phys. Rev. Lett.*, 1998, **27**, 3867.
7 A. S. Al-Shahrany, D. Bradley, M. Lawes, K. Liu and R. Woolley, *Combust. Sci. Technol.*, 2006, **178**, 1771.
8 I. M. Naboko, N. M. Rubtsov, B. S. Seplyarskii, V. I. Chernysh and G. I. Tsvetkov, *Mendeleev Commun.*, 2013, **23**, 163.
9 N. M. Rubtsov, B. S. Seplyarskii, K. Ya. Troshin, V. I. Chernysh and G. I. Tsvetkov, *Mendeleev Commun.*, 2011, **21**, 218.
10 N. M. Rubtsov, B. S. Seplyarskii, K. Ya. Troshin, V. I. Chernysh and G. I. Tsvetkov, *Mendeleev Commun.*, 2012, **22**, 222.
11 B. Lewis and G. Von Elbe, *Combustion, Explosions and Flame in Gases*, Academic Press, New York, London, 1987.
12 K. Kristoffersen, *Gas Explosions in Process Pipes*, Dr. Ing. Thesis, Faculty of Technology, Telemark University College, Porsgrunn, Norway, 2004.
13 I. M. Naboko, N. M. Rubtsov, B. S. Seplyarskii, K. Ya Troshin, G. I. Tsvetkov and V. I. Chernysh, *Mendeleev Commun.*, 2013, **23**, 358.
14 V. Akkerman, V. Bychkov, A. Petchenko and L.-E. Eriksson, *Combust. Flame*, 2006, **145**, 675.
15 P. Clavin, *Annu. Rev. Fluid Mech.*, 1994, **26**, 321.
16 C. Clanet, G. Searby and P. Clavin, *J. Fluid Mech.*, 1999, **385**, 157.
17 A. Majda, *Equations for Low Mach Number Combustion*, Center of Pure and Applied Mathematics, University of California, Berkeley, 1982, PAM-112.
18 F. Nicoud, *J. Comput. Phys.*, 2000, **158**, 71.

Received: 6th November 2013; Com. 13/4241